An Update to the Canadian Shield Stress Database

NWMO-TR-2015-18 September 2015

Salina Yong and Sean Maloney
MIRARCO

nwmo
NUCLEAR WASTE MANAGEMENT ORGANIZATION
SOCIÉTÉ DE GESTION DES DÉCHETS NUCLÉAIRES

Nuclear Waste Management Organization
22 St. Clair Avenue East, 6th Floor
Toronto, Ontario
M4T 2S3
Canada

Tel: 416-934-9814
Web: www.nwmo.ca

An Update to the Canadian Shield Stress Database

NWMO-TR-2015-18

September 2015

Salina Yong and Sean Maloney
MIRARCO

Document History

Title:	An Update to the Canadian Shield Stress Database		
Report Number:	NWMO-TR-2015-18		
Revision:	R000	Date:	September 2015
MIRARCO			
Authored by:	Salina Yong and Sean Maloney		
Verified by:	Sean Maloney and Peter Kaiser		
Approved by:	Sean Maloney		
Nuclear Waste Management Organization			
Reviewed by:	Tom Lam		
Accepted by:	Mark Jensen		

ABSTRACT

Title: **An Update to the Canadian Shield Stress Database**
Report No.: **NWMO-TR-2015-18**
Author(s): Salina Yong and Sean Maloney
Company: MIRARCO
Date: September 2015

Abstract

This report provides an update of the 2005 state of ground stress report for the Ontario portion of the Canadian Shield. A database of 304 stress measurements has been assembled that includes 75 new measurements since 2005. The database covers a range of depths between 12 and 2,552 m below ground surface with measurement data obtained largely from operating mines in Ontario. A data screening process was followed that involved 5 acceptance criteria to assess quality and reduce uncertainty when establishing representative ground stress state equations. As a result of the data screening, the database supporting the analysis in this study was reduced to 199 entries.

Consistent with past studies, the state of ground stress in Shield terrain is sub-divided into 3 Zones: i) the stress-relaxed zone (Domain 1; 0-300m); ii) the transitional zone (Domain 2; 300 – 600 m); iii) the undisturbed zone (Domain 3; 600-1500m). The best-fit relationships are developed for Domains 1 and 3 as evidence suggests the interpretations are robust and less sensitive to site specific conditions. Variability and uncertainty is highest in transitional stress Domain 2, which reveals a strong dependency on the local geologic setting. As recommended in 2005, stresses in Domain 2 can be assumed to increase linearly between Domains 1 and 3 for preliminary modelling and sub-surface design purposes.

While this review has provided insight on the stress state within in the crystalline rocks of the Canadian Shield, direct measurements of ground stress magnitudes and orientations are required to provide site-specific estimates that further constrain stress state and reduce uncertainty.

TABLE OF CONTENTS

LIST OF TABLES

LIST OF FIGURES

1. INTRODUCTION

As part of the Deep Geologic Repository Technology Program (DGRTP) MIRARCO undertook a study to compile in-situ stress measurement data for the Canadian Shield (Kaiser and Maloney, 2005). These data were then used to examine the spatial state of ground stresses in the Canadian Shield through: i) the interpretation of ground stress domains as a function of depth; and ii) illustrative equations to predict ground stress magnitude within each stress domain. This study, conducted under the Adaptive Phased Management (APM) Program, provides an update of the 2005 review that incorporates the results of new stress measurement data on the Ontario portion of the Canadian Shield gathered since that time.

In-situ stresses in the ground are rarely uniform. Their distribution depends on a number of factors such as rock mass characteristics (i.e., heterogeneities, fabric, discontinuities, geological structure, etc.) and the site loading history (e.g., tectonic activity, erosion and/or glaciation). The end result is that local stresses may bear little semblance to the general or average stress state. Consequently, the contribution of these various factors to the measured stress state must be understood if the measurements are to be used with confidence. According to Amadei and Stephansson (1997), in-situ stresses can only be determined with an error of ±10-20% under ideal conditions. For engineering purposes, it is necessary to establish reliable and average stress boundary conditions along with the associated ranges of variability and uncertainty.

Extensive mineral resources throughout the region, as well as, the need to design and operate deep underground mines have been the basis of the measurement of ground stresses in the Canadian Shield. Most of the published data have been acquired from mining operations in Ontario, Manitoba, and Quebec using various methods in different geological settings. As a result, some measurements may have been made at locations that have been affected by mining activities, such as near underground excavations, while others have been impacted by core damage in high stress environments. This has resulted in a database where stress magnitudes and orientations exhibit considerable scatter. As part of this updated review, acceptance criteria were developed to screen the stress measurement data set so as to select estimates of increased quality and to reduce uncertainty in the characterisation of depth dependent ground stress states.

2. SCOPE

This review as involved a number of activities to provide a thorough up-date and re-assessment of the state of ground stresses on the Ontario portion of the Canadian Shield. Initial activities included the development of an on-line survey that was distributed to discussion groups and organizations to identify and contact potential sources with post-2005 stress measurement data. Following receipt and assembly of the new measurement data they were added to the existing 2005 database, which then was entirely vetted with new acceptance criteria to assess quality. The resulting screened data base was then used to establish depth dependent stress domains and develop illustrative equations with which to predict stress magnitude in these domains. Details regarding these various activities are discussed in the following sections.

3. STRESS MEASUREMENT DATA

The merging of the 2005 database (229) with new post-2005 data (75) acquired through the on-line survey process created a total of 304 entries. The new post-2005 data was provided exclusively by operating mines. While the 2005 database considered measurement data from four geological provinces (Superior, Southern, Churchill, and Grenville), this update considers only those made in the Superior and Southern provinces as shown in Figure 1.

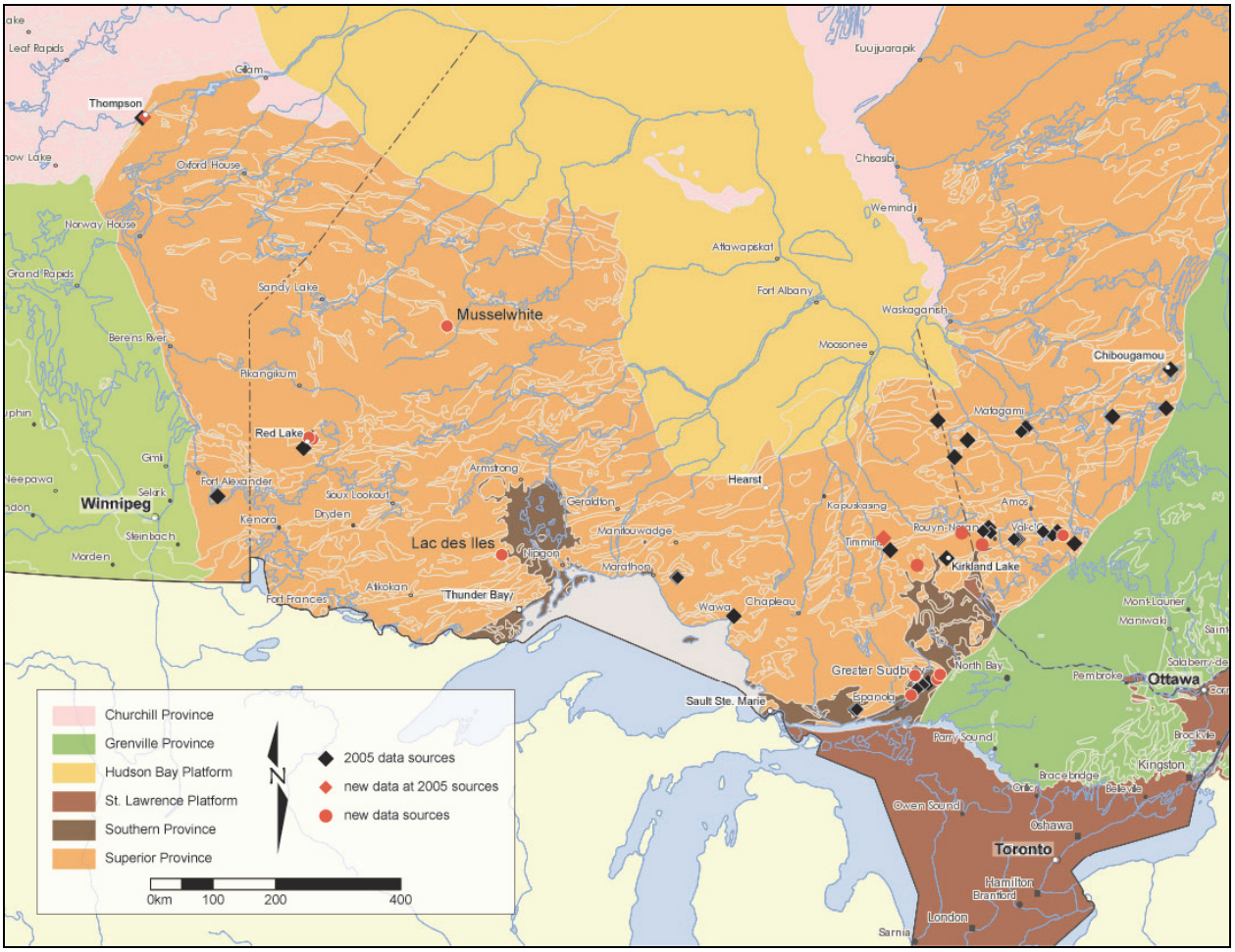

Figure 1: Locations of Data Sources in the Superior and Southern Geological Provinces of Canada (base map courtesy of Natural Resources Canada, 2009)

3.1 DATABASE QUALITY ASSESSMENT

When reviewing the database, it was noticed that some entries did not include orientation data, three orthogonal (whether principal or Cartesian space) stress magnitudes, or the vertical stress determined by the measurement campaign. This led to the development of the acceptance criteria to select data for inclusion in the final database. The acceptance criteria are:

1) magnitudes and orientations for three orthogonal stresses, which allowed for transformation into Cartesian space;
2) data interpretation within limitations of measurement technique (e.g., results eliminated when obviously impacted by epoxy softening or uncorrected for significant temperature effects for campaigns involving the CSIRO HI cell);
3) normality (±0.1) and orthogonality (±0.1) of principal stress directional cosines;
4) discrepancy (±15%) between the reported and transformed vertical stress magnitude; and
5) stress ratios (±2 standard deviations).

The quality of the combined database was assessed in two stages with the first involving elimination of entries based on the first two criteria above. The deduced stress state was reported as three components within an orthogonal framework (i.e., either principal or Cartesian) in the majority of tests. In the current analysis, the second criterion was only applied to select campaigns of the newly acquired (i.e., post-2005) data. Specifically, two campaigns were selected due to the lack of nearby measurements: Musselwhite and Lac des Iles. In both cases, MIRARCO was the contractor involved and therefore, all data and relevant contextual information was readily accessible for closer examination and re-processing of the strain data. This first assessment stage resulted in the elimination of 52 entries.

The second assessment stage encompassed data elimination based on the last three criteria. Normality was assessed through calculation of the unit vector of each principal stress component while orthogonality was assessed through the calculation of the dot products of the three principal stress directional cosines. Because the first assessment stage eliminated data with incomplete stress state characteristics, all remaining data entries provided the required information for transformation from principal to Cartesian space. The transformed vertical stress component was then compared against reported values where available. The majority of entries differed by less than 0.5% and this small difference is illustrated in Figure 2. The last criterion examined inconsistencies in the data based on ratios of the principal stress magnitudes transformed into Cartesian space. Consistency in the database appeared to be best constrained by the ratio of the two horizontal stresses (rightmost plot in Figure 3). This second and final assessment stage resulted in the elimination of a further 25 entries.

Elimination of non-compliant data based on the above criteria reduces the updated 2015 database to a total of 199 entries, consisting of 173 from the 2005 database and 26 newly acquired (APPENDIX A). This database covers depths ranging from 12 to 2,552 m with sites distributed as illustrated in Figure 4. Where possible, the data presented in this report distinguishes between the 2005 and post-2005 reviews.

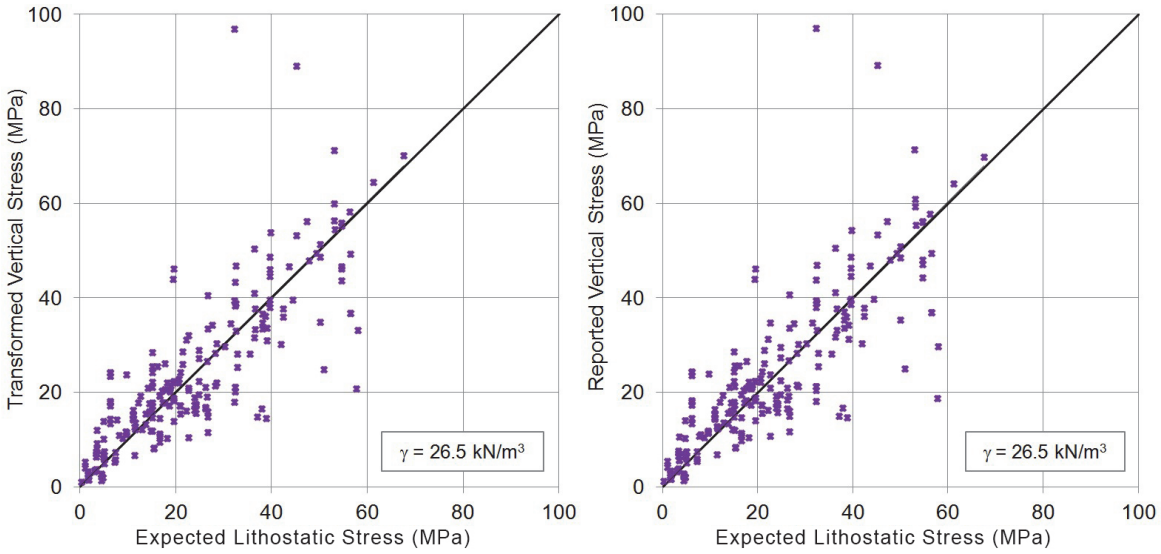

Figure 2: Transformed (left) and Reported (right) Vertical Stress Compared to Expected Overburden Stress

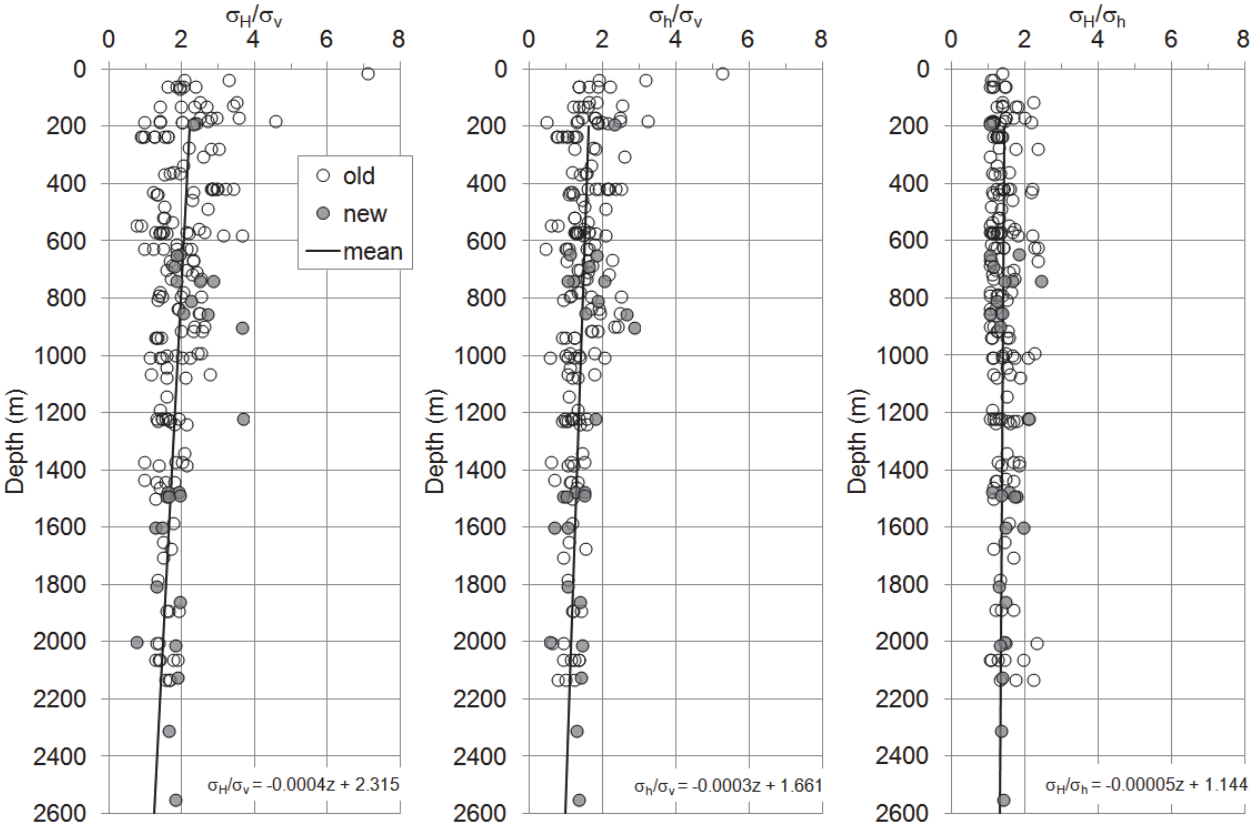

Figure 3: Ratios of Principal Stress Magnitudes Transformed into Cartesian Space (σ_H is the maximum horizontal, σ_h is the minimum horizontal, and σ_v is the vertical)

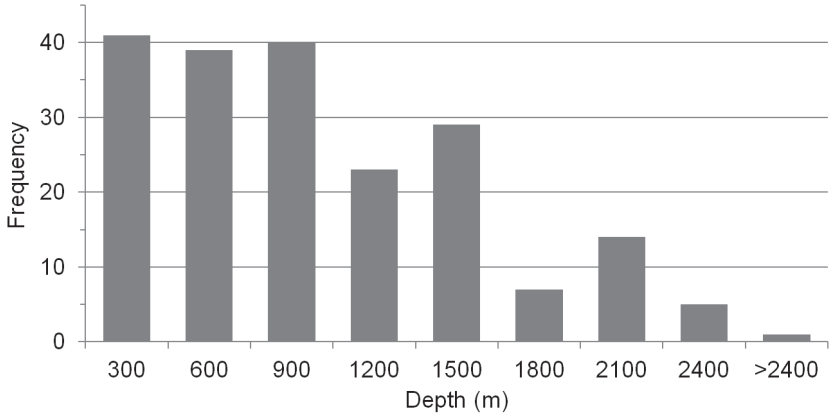

Figure 4: Depth Distribution of Updated 2015 Stress Measurements

3.2 DATABASE ANALYSIS

Analysis of the updated 2015 database entailed the development of best-fit relationships, relative to depth, for the three Cartesian stress components as the principal stress components are somewhat likewise aligned (demonstrated in Section 4.1). Relationships have been defined for the entire database as a whole and also by separating the data into the two geological provinces, as well as, into four depth domains. Following Kaiser and Maloney (2005), Domain 1 (0 to 300 m) is stress-relaxed or disturbed, largely due to movement along local flat-lying geological structures. Domain 2 (300 to 600 m) represents the transition between the overlying relaxed/disturbed domain and the underlying undisturbed domain. Domain 3 (600 to 1,500 m) is considered “undisturbed” as it is generally defined by regional fault structures and stress history (i.e., tectonic stress, glaciations, erosion, etc.). Below 1,500 m, the database is comparatively sparse; consequently, no relationship is defined for Domain 4. As well, owing to its transitional nature, relationships have not been defined for Domain 2.

As Figure 2 demonstrated, the transformed vertical stress component compares well with the expected litheostatic stress (calculated based on a generic unit weight of 26.5 kN/m^3). This is further supported by a linear regression of all the data (Figure 5) with a slope of 0.97 and a corresponding coefficient of determination (R^2) of 0.8. The transformed vertical stress was used in lieu of the reported due to the earlier noted discrepancy and for consistency since the transformed value guarantees the normality and orthogonality of the principal stress components. The first step in developing the best-fit relationships was to further reduce the database through removal of entries beyond two standard deviations (i.e., 95% confidence interval).

The remaining database was then separated into two groups based on their standard deviation from the trendline shown in Figure 5. In an attempt to provide the best possible relationships, linear regressions considered only data within one standard deviation. The box in Figure 6 shows that one standard deviation (68% confidence interval) constrains the dataset to deviations of less than 50% between the transformed vertical and expected overburden stress. In Figure 7, the best-fit regressions from one and two standard deviations are compared and illustrate that the reduction in the data population does not adversely impact the relationship. However, refinement of the relationship, defined with a sample size of one deviation, improves both the correlation (indicated by a 6% increase in R^2) and expected null value when projected to surface.

Although this approach appears to improve the best-fit linear regression, variability would be misrepresented if determined in the same manner. The standard deviation of each best-fit relationship reported in Section 4 is ascertained by considering the entire vetted 2015 stress database.

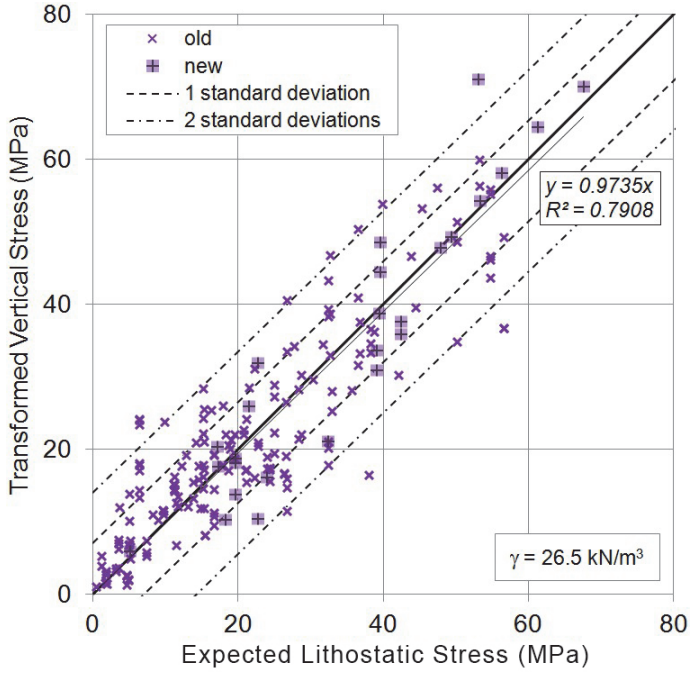

Figure 5: Constraining the 2015 Database for Developing Best-fit Relationships

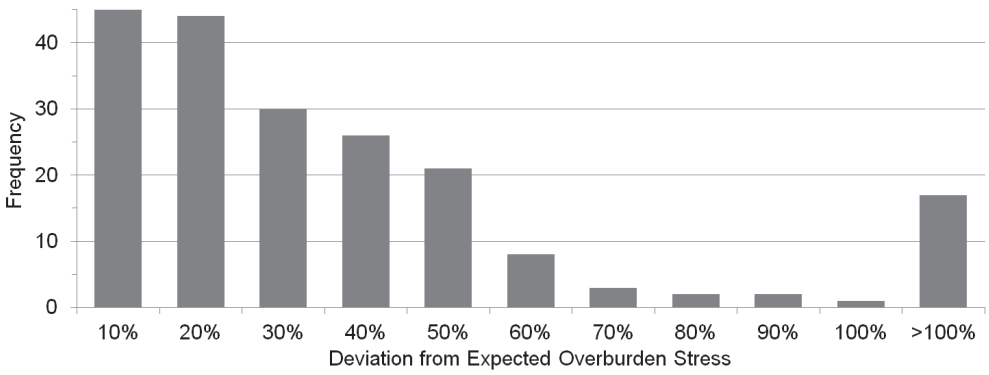

Figure 6: Distribution of Transformed Vertical Stress Deviation

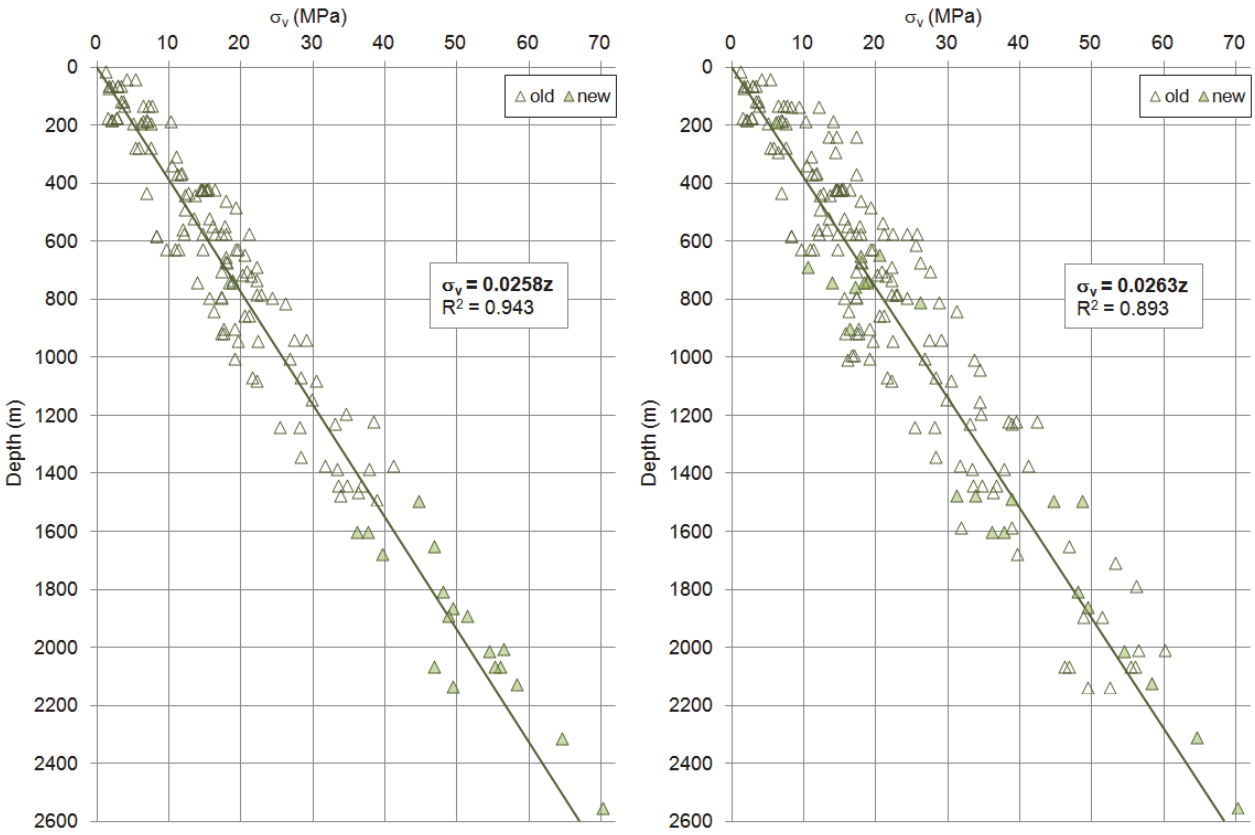

Figure 7: Linear Regression of Vertical Stress Data within One Standard Deviation (left) and Two Standard Deviations (right) of the Best-fit Trendline Defined in Figure 5

4. RECOMMENDED IN-SITU STRESS STATE

Recommendations for the in-situ stress state in the Ontario portion of the Canadian Shield are presented in two coordinate systems in this section. The relationships developed for the principal stress space are more general since they consider the entire 2015 updated database with no distinction made for the geological provinces or depth domains. Conversely, relationships developed for the Cartesian space are separated into the two geological provinces, Superior and Southern, and three stress domains.

4.1 PRINCIPAL STRESS STATE

The principal stress orientations for the updated 2015 database are plotted in Figure 8 and demonstrate that the principal stresses are somewhat aligned with Cartesian axes where the major and intermediate principal stresses are sub-horizontal whereas the minimum stress is sub-vertical. The average maximum principal stress trends WSW-ENE, which is consistent with the major trend indicated in the World Stress Map database for the study area (Reinecker et al. 2004). The direction of the minor principal stress appears to be well-constrained whereas the intermediate principal stress direction appears to be the most variable.

The principal stress magnitudes are plotted in Figure 9 along with the best-fit relationships and 95% confidence derived from data within one standard deviation of agreement between the transformed vertical and expected overburden stresses (Figure 5). Although the relationships, listed in Table 1, have been deduced from the 2015 updated database as a whole, it is apparent from the plots of the major and intermediate principal stresses that two to three depth domains exist. Such domain grouping is more difficult to discern in the minor principal stress magnitudes. The domains are more apparent when examining the principal stress ratios plotted in Figure 10. Below 200 m depth, the σ_1/σ_3 and σ_2/σ_3 ratios are dominated by a linear trend while a gradual turn towards an asymptote is evident between 200 and 300 m. While scatter exists from a depth of 300 to 1,000 m, a clear linear trend is discernible in the ratios at depths of 600 m and greater.

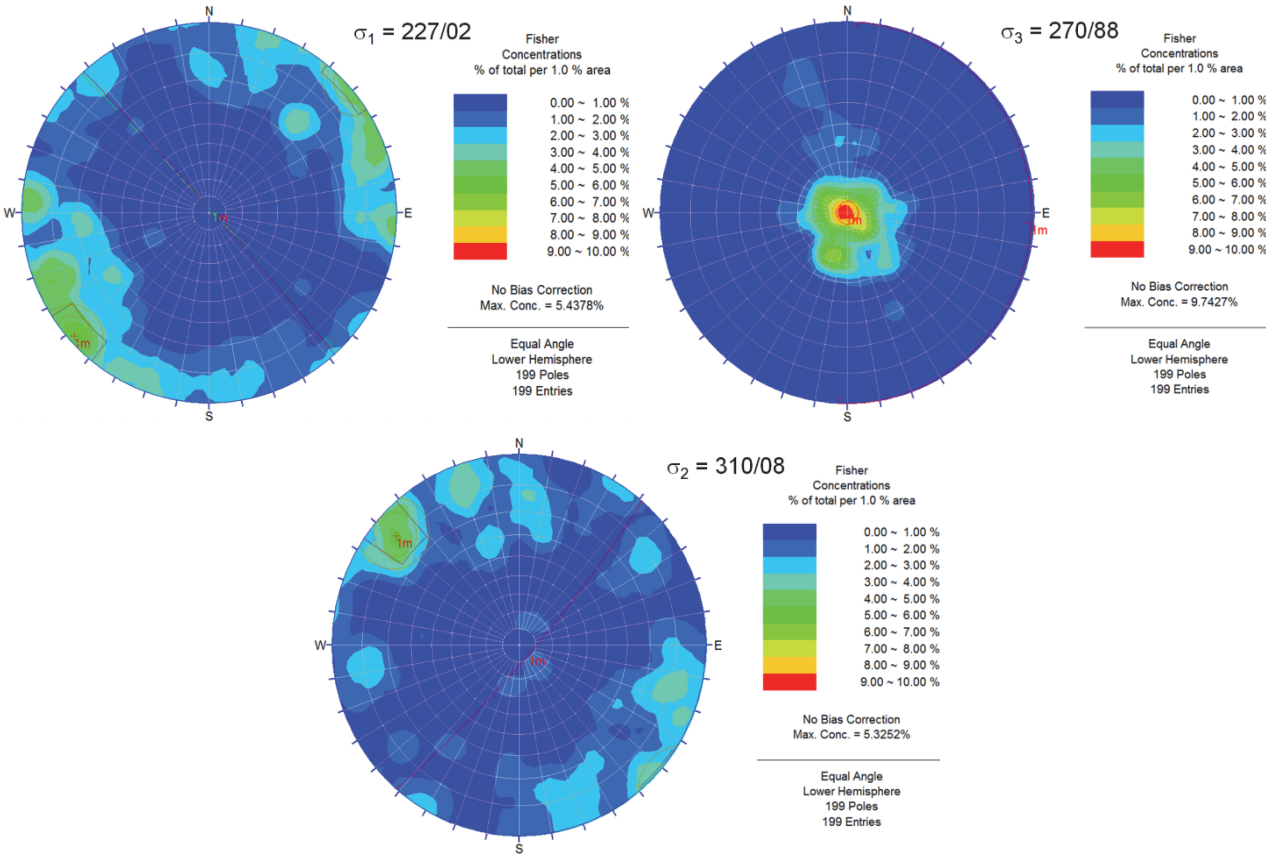

Figure 8: Distribution of Principal Stress Orientations of the 2015 Updated Database with Average Directions Indicated

Table 1: Best-fit Relationships for Principal Stress (all domains)

2015 Update
σ_1 (MPa) = (0.040±0.001)z* - (9.185±1.500)
σ_2 (MPa) = (0.029±0.001)z* + (4.617±1.159)
σ_3 (MPa) = (0.021±0.001)z* - (0.777±0.872)

*depth in metres

Comparison with the best-fit relationships determined from the 2005 review are summarised in Table 2 to Table 3 and plotted in Figure 11. The results are similar with a larger difference in the relationships developed for the stress-relaxed Domain 1. This is a direct result of the quality assessment undertaken in this update. The smaller differences in the undisturbed Domain 3 are related to the additional data included in this update study and show that the relationships are consistent and better constrained.

Comparison of the major and minor principal stress orientations (Table 4) also indicates similarities between the two reviews (Figure 12 and Figure 13). The differences in orientations of Domain 1 are small despite a larger difference in the best-fit magnitude relationships (Figure 11). This shows that although there is greater uncertainty in determining the magnitudes, the orientations are fairly consistent in the stress-relaxed Domain 1. A larger difference in the major principal stress is shown in the undisturbed Domain 3 and this is attributed to the addition of data in the current review. However, the difference is a shift in concentration between the two largest sets of orientation data, which appear in both reviews. Hence, two sets of orientations (30° apart in azimuth) for the major principal stress may naturally exist. Both sets are in line with the World Stress dominant orientation of WSW for this region. The minor principal in both domains is vertical and well constrained.

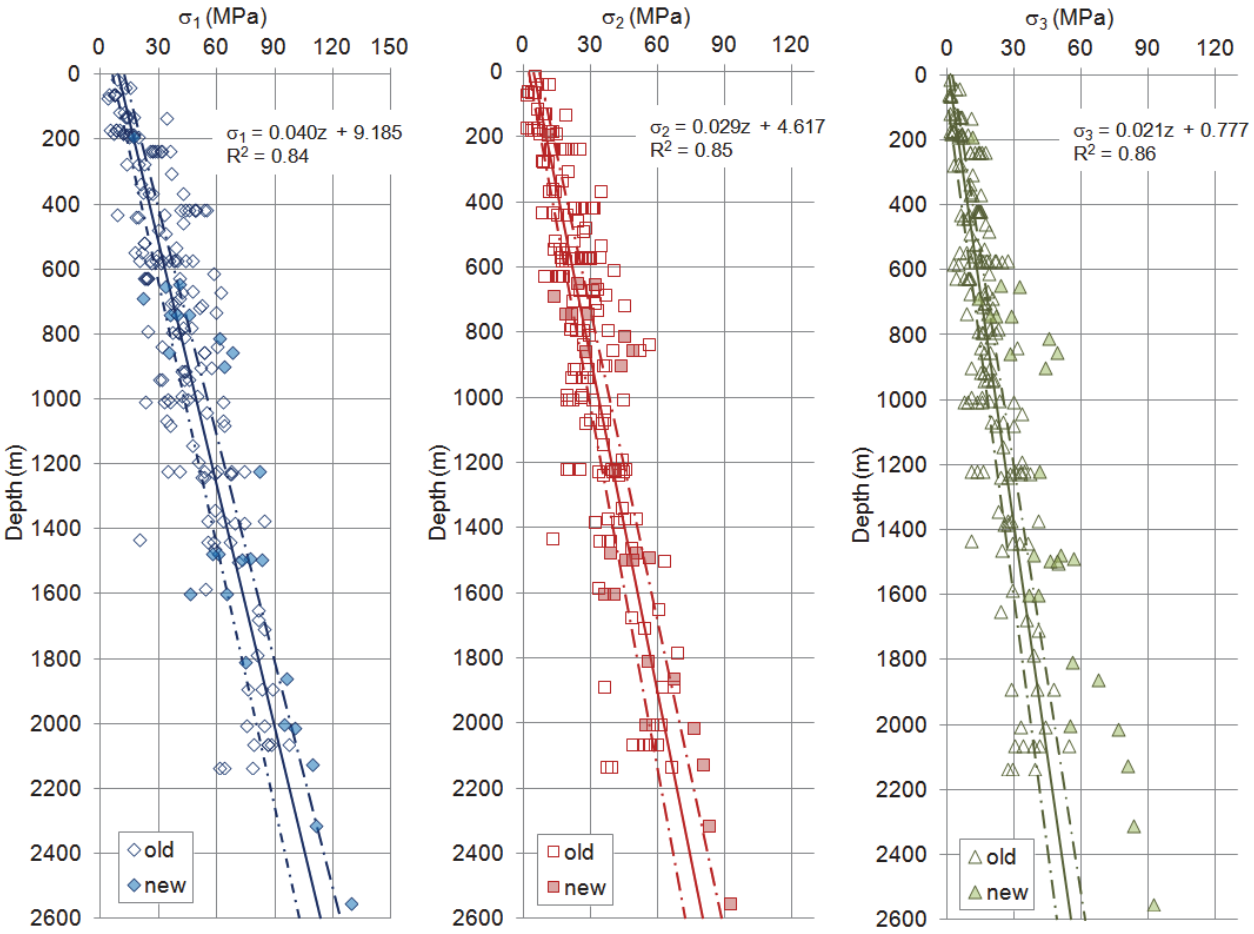

Figure 9: Principal Stress Data and Best-fit Relationships for the 2015 Updated Database (all domains)

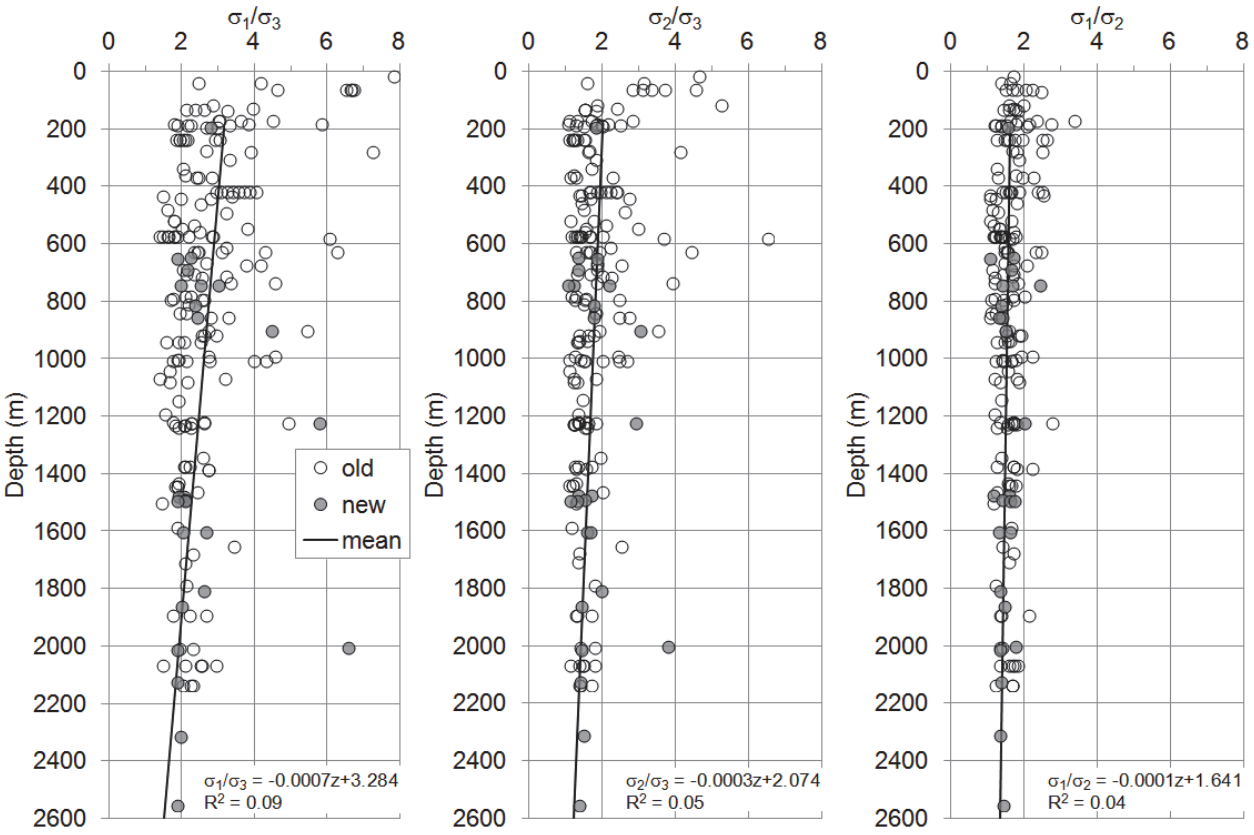

Figure 10: Principal Stress Ratios for the 2015 Updated Database (all domains)

Table 2: Comparison of Domain 1 Magnitudes with 2005 Review

2015 Update	2005 Review
σ_1 (MPa) = (0.038±0.010)z* + (6.318±1.609)	σ_1 (MPa) = (0.071±0.019)z* + (5.768±3.358)
σ_2 (MPa) = (0.019±0.008)z* + (4.349±1.320)	σ_2 (MPa) = (0.043±0.015)z* + (3.287±2.600)
σ_3 (MPa) = (0.021±0.001)z* - (0.777±0.872)	σ_3 (MPa) = (0.034±0.005)z*

*depth in metres

Table 3: Comparison of Domain 3 Magnitudes with 2005 Review

2015 Update	2005 Review
σ_1 (MPa) = (0.038±0.004)z* + (11.052±4.437)	σ_1 (MPa) = (0.026±0.012)z* + (23.636±11.556)
σ_2 (MPa) = (0.024±0.003)z* + (8.991±3.465)	σ_2 (MPa) = (0.016±0.010)z* + (17.104±10.538)
σ_3 (MPa) = (0.021±0.001)z* - (0.777±0.872)	σ_3 (MPa) = (0.020±0.008)z* + (1.066±8.247)

*depth in metres

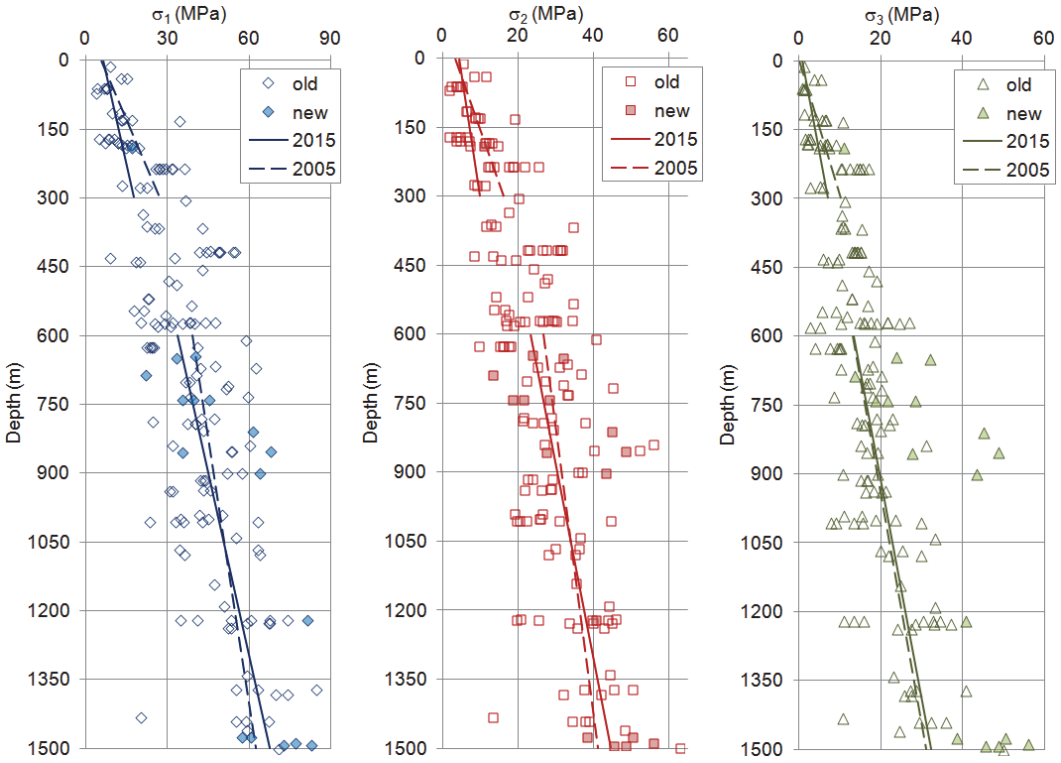

Figure 11: Principal Stress Best Fit Comparisons between 2005 Review and 2015 Update (Domain 1 and 3)

Table 4: Comparison of Principal Stress Orientations (trend/plunge) with 2005 Review

	2015 Update	2005 Review
Domain 1		
σ_1	212/02	039/02
σ_3	112/81	347/85
Domain 3		
σ_1	275/02	249/03
σ_3	236/85	134/83

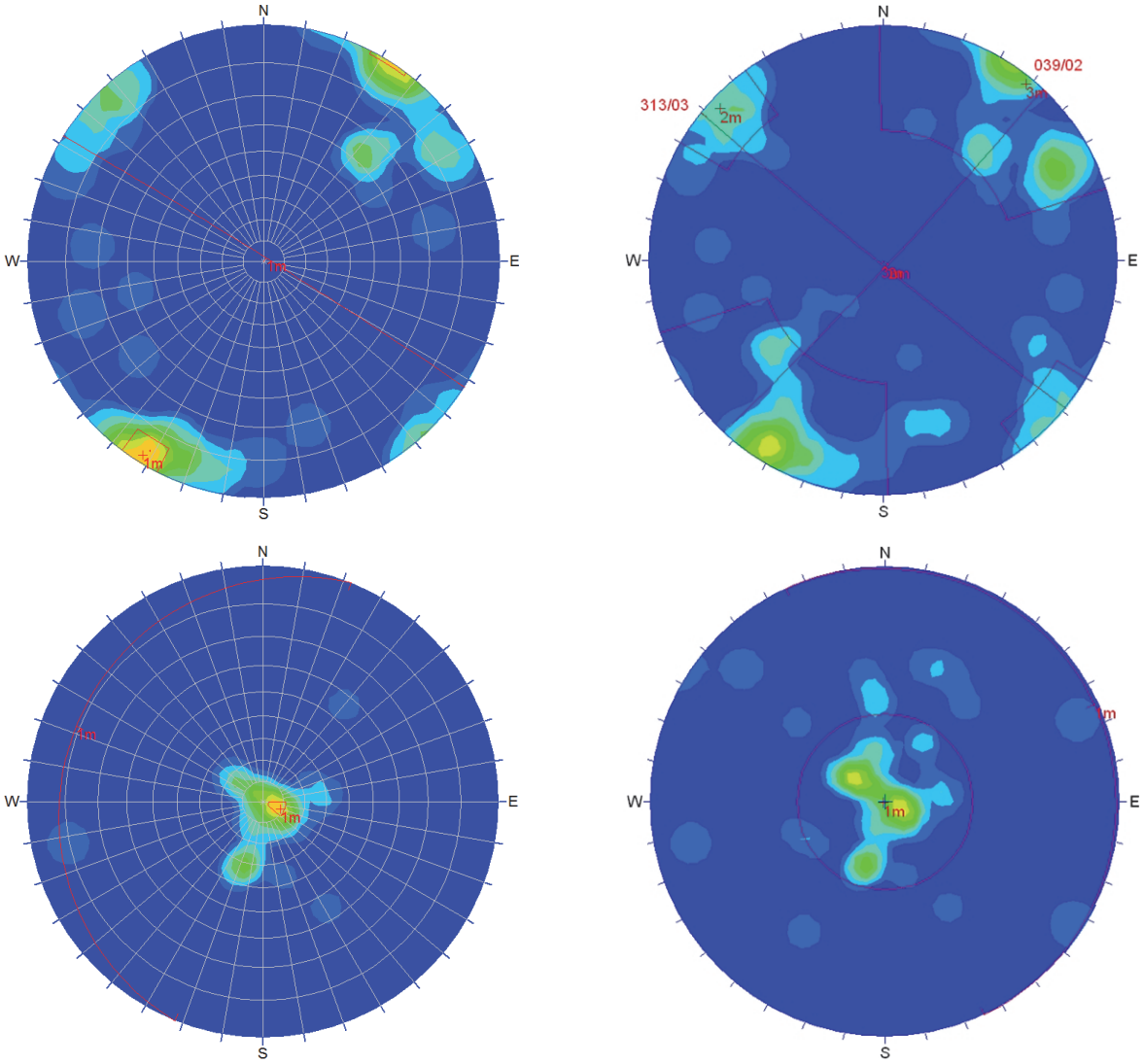

Figure 12: Principal Stress Orientation (major in top and minor in bottom) Comparisons between 2015 Update (left) and 2005 Review (right) for Domain 1

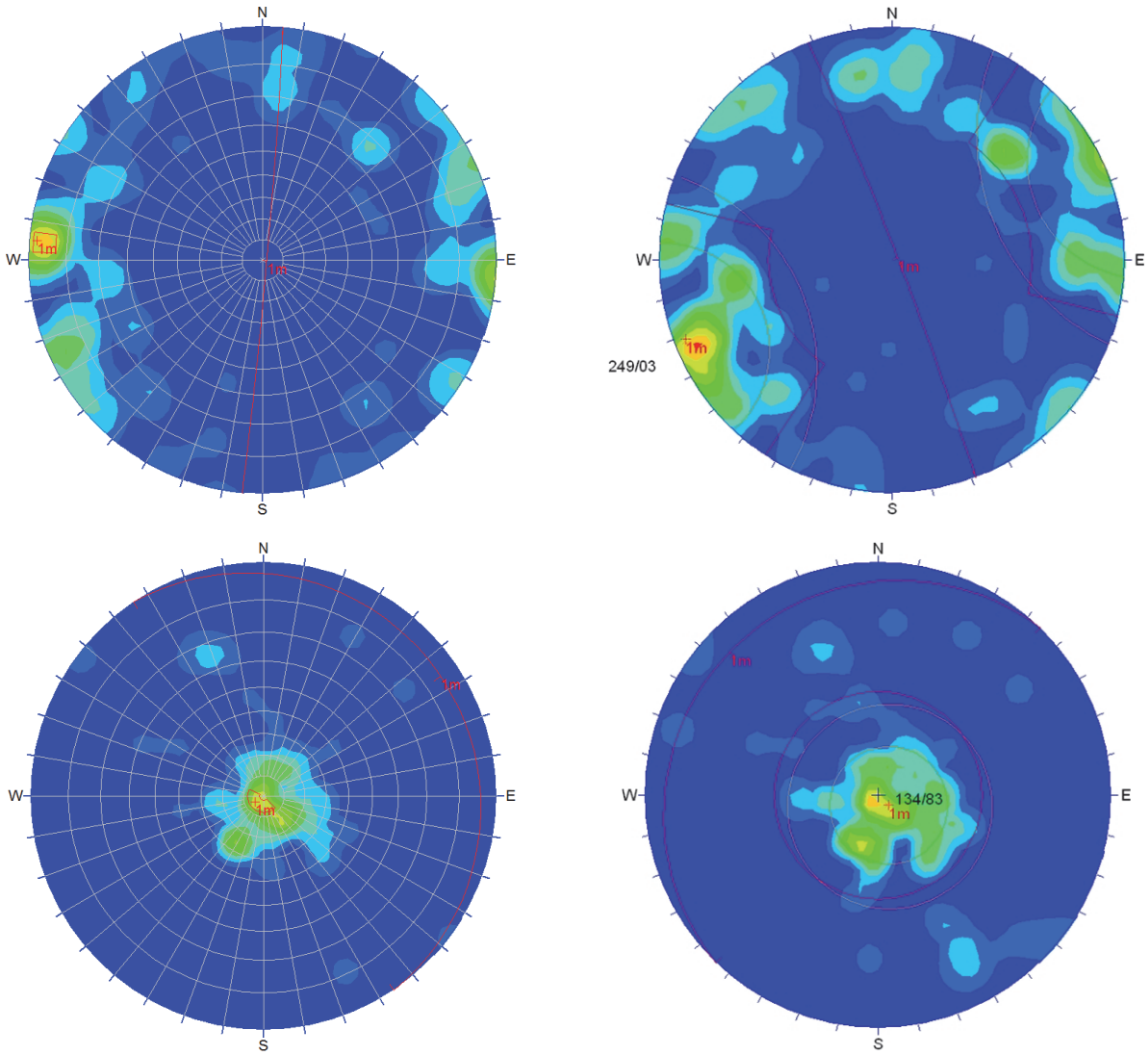

Figure 13: Principal Stress Orientation (major in top and minor in bottom) Comparisons between 2015 Update (left) and 2005 Review (right) for Domain 3

4.2 CARTESIAN STRESS STATE

In Cartesian space, the 2015 updated database and corresponding best-fit relationships for depth Domains 1 and 3 are summarised in Table 5 and plotted in Figure 14. The associated stress ratios are plotted in Figure 3. The relationships for Domain 1 required consideration of the entire 2015 updated database unlike those developed for Domain 3 (see Section 3.2). This emphasises the greater disturbed nature of the upper 300 m, which can be attributed to the greater weakening impact of near-surface geological processes on both the structure and material properties of this domain.

The best-fit linear regressions and corresponding stress ratios for the Superior Province are plotted in Figure 15 and Figure 16, respectively. Table 6 summarises the best-fit relationships developed for Domains 1 and 3. Again, Domain 1 regressions required consideration of the

entire 2015 updated database unlike those developed for Domain 3 (see Section 3.2). This is not surprising since all data in Domain 1 are for sites located in the Superior Province.

Table 5: Best-fit Relationships for Horizontal and Vertical Stress (entire 2015 Updated Database)

Domain 1	Domain 3
σ_H (MPa) = (0.060±0.027)z* + (3.722±4.659)	σ_H (MPa) = (0.035±0.005)z* + (9.500±5.373)
σ_h (MPa) = (0.044±0.022)z* + (2.981±3.766)	σ_h (MPa) = (0.024±0.005)z* + (8.883±4.867)
σ_v (MPa) = (0.026±0.001)z*	

*depth in metres

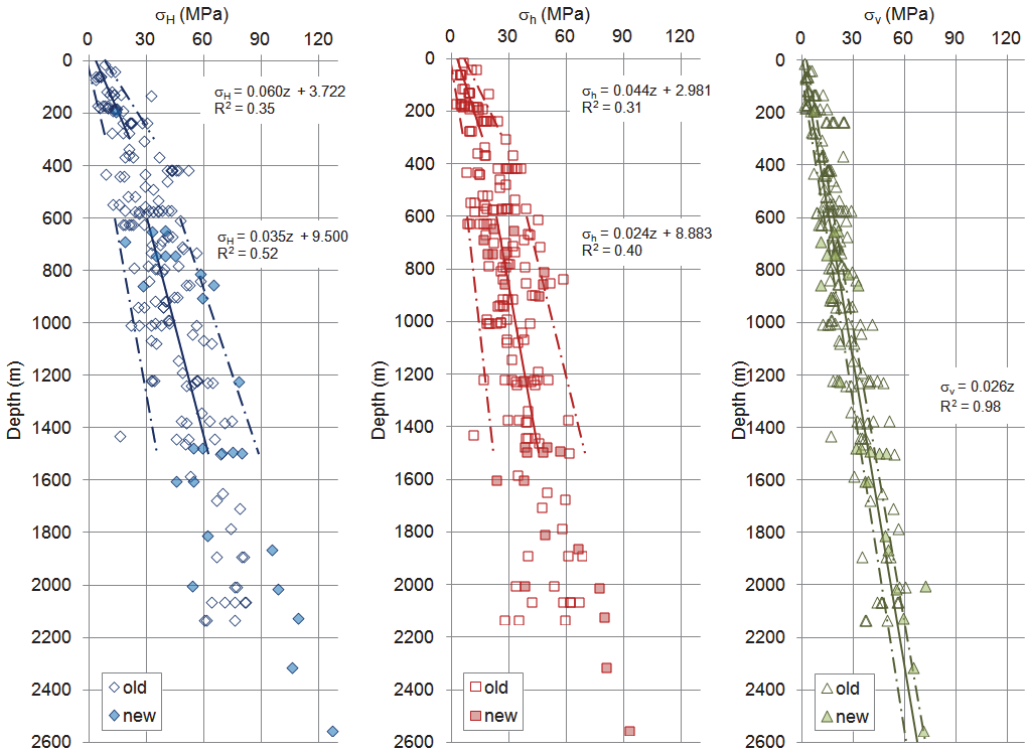

Figure 14: Horizontal and Vertical Stress Data and Best-fit Relationships for the entire 2015 Updated Database with Variability Represented by 95% Confidence Intervals (Two Standard Deviations)

Table 6: Best-fit Relationships for Horizontal and Vertical Stress (Superior Province)

Domain 1	Domain 3
σ_H (MPa) = (0.060±0.027)z* + (3.722±4.659)	σ_H (MPa) = (0.030±0.003)z* + (14.303±2.728)
σ_h (MPa) = (0.044±0.022)z* + (2.981±3.766)	σ_h (MPa) = (0.022±0.002)z* + (11.196±2.310)
σ_v (MPa) = (0.026±0.001)z*	

*depth in metres

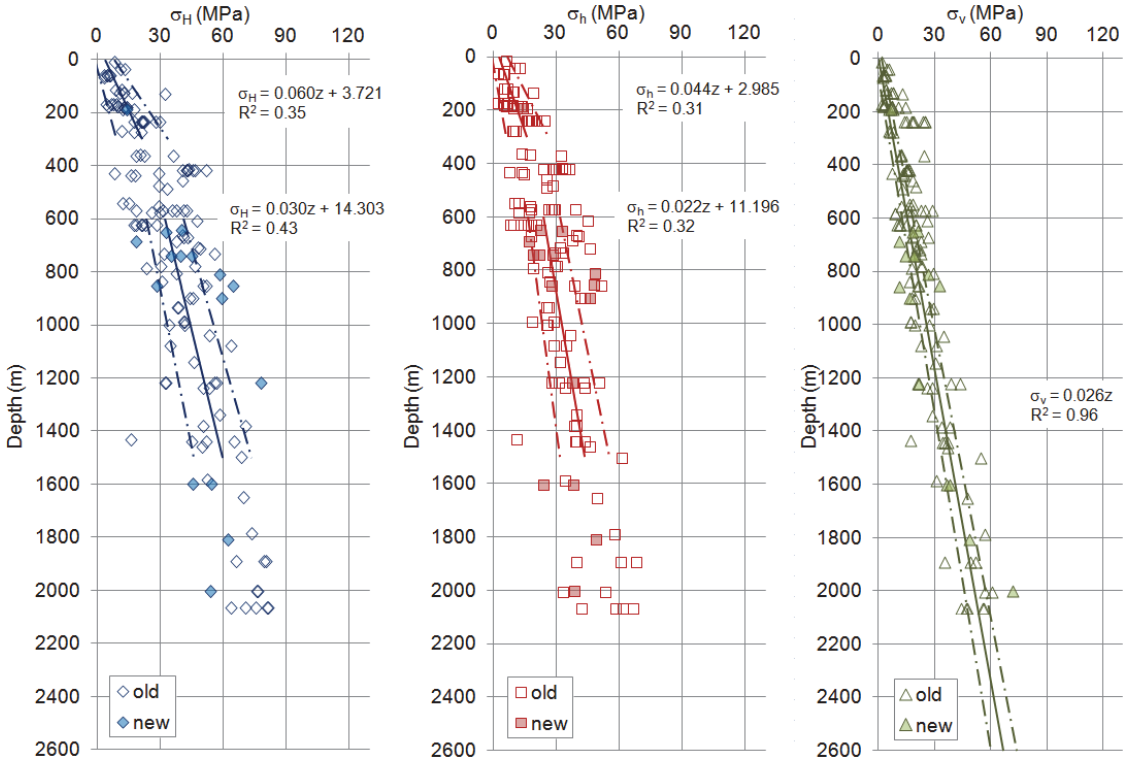

Figure 15: Horizontal and Vertical Stress Data and Best-fit Relationships for the Superior Province with variability represented by 95% confidence intervals (two standard deviations)

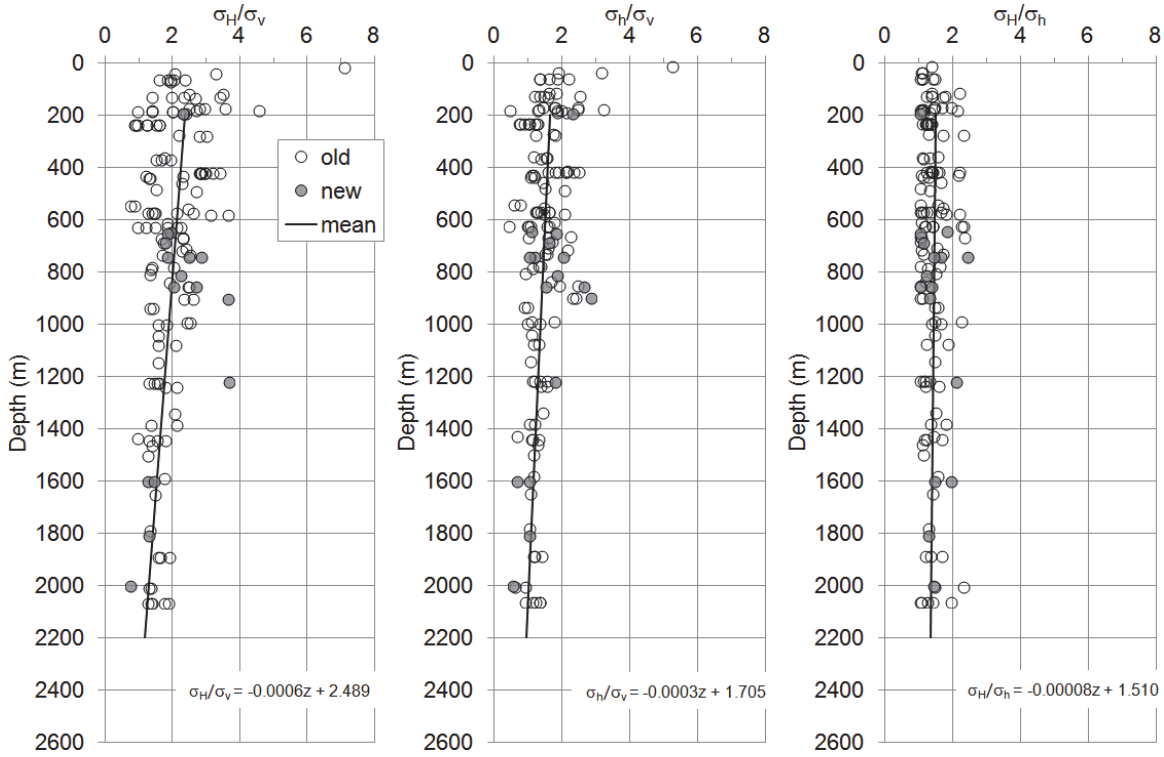

Figure 16: Horizontal and Vertical Stress Ratios for the Superior Province

Less data was available for the Southern Province: 51 entries compared to 148 entries for the Superior Province. As a result, regression of best-fit relationships is only possible in Domain 3 for the two horizontal stress components (Figure 17; Table 7). The corresponding stress ratios are plotted in Figure 18. These plots show well-constrained relationships, which is likewise illustrated by the higher coefficient of determination (R^2) for the two horizontal stresses. Projection of the best-fit relationship for the vertical stress nearly intersects zero at ground surface and its slope is close to that of the generic rock unit weight (γ = 26.5 kN/m^3) used to determine the expected lithostatic stress. This is consistent with the notion that Domain 3 is the least disturbed by near-surface geological processes.

Table 7: Best-fit Relationships for Horizontal and Vertical Stress (Southern Province)

Domain 3
σ_H (MPa) = (0.049±0.003)z* - (5.940±3.090)
σ_h (MPa) = (0.030±0.003)z* + (3.208±2.939)
σ_v (MPa) = (0.026±0.002)z*

*depth in metres

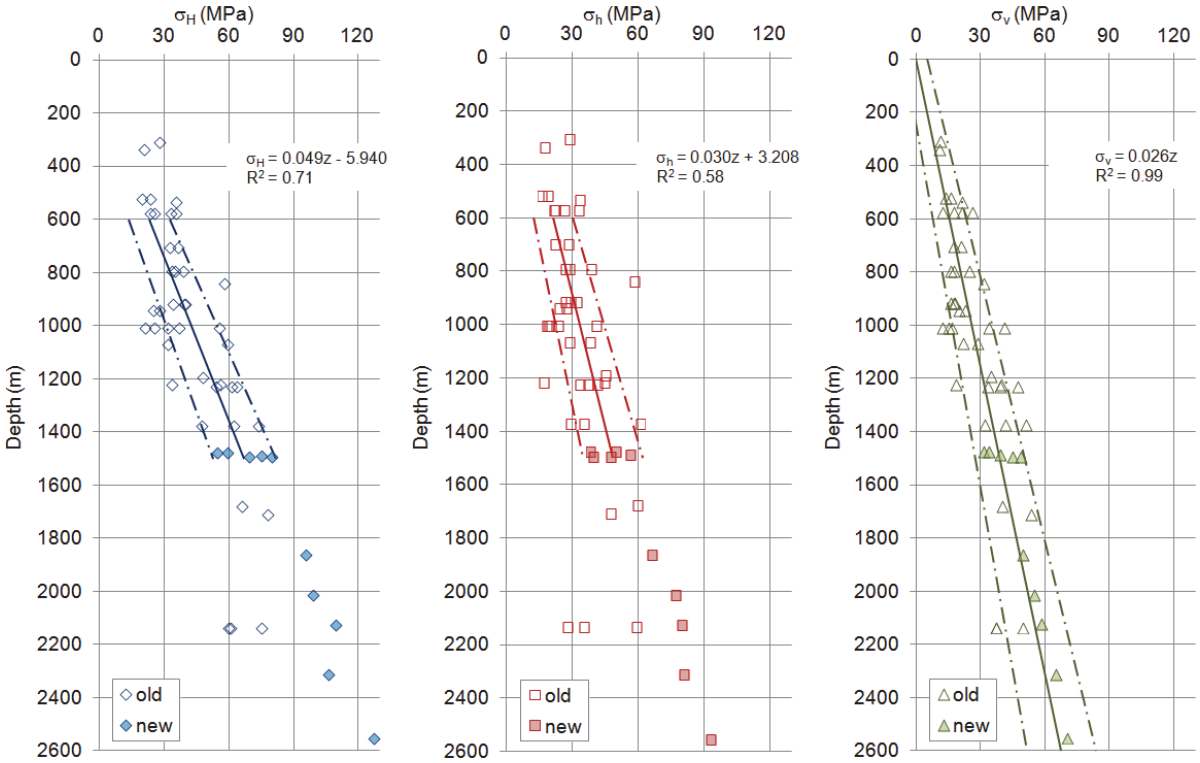

Figure 17: Horizontal and Vertical Stress Data and Best-fit Relationships for the Southern Province with variability represented by 95% confidence intervals (two standard deviations)

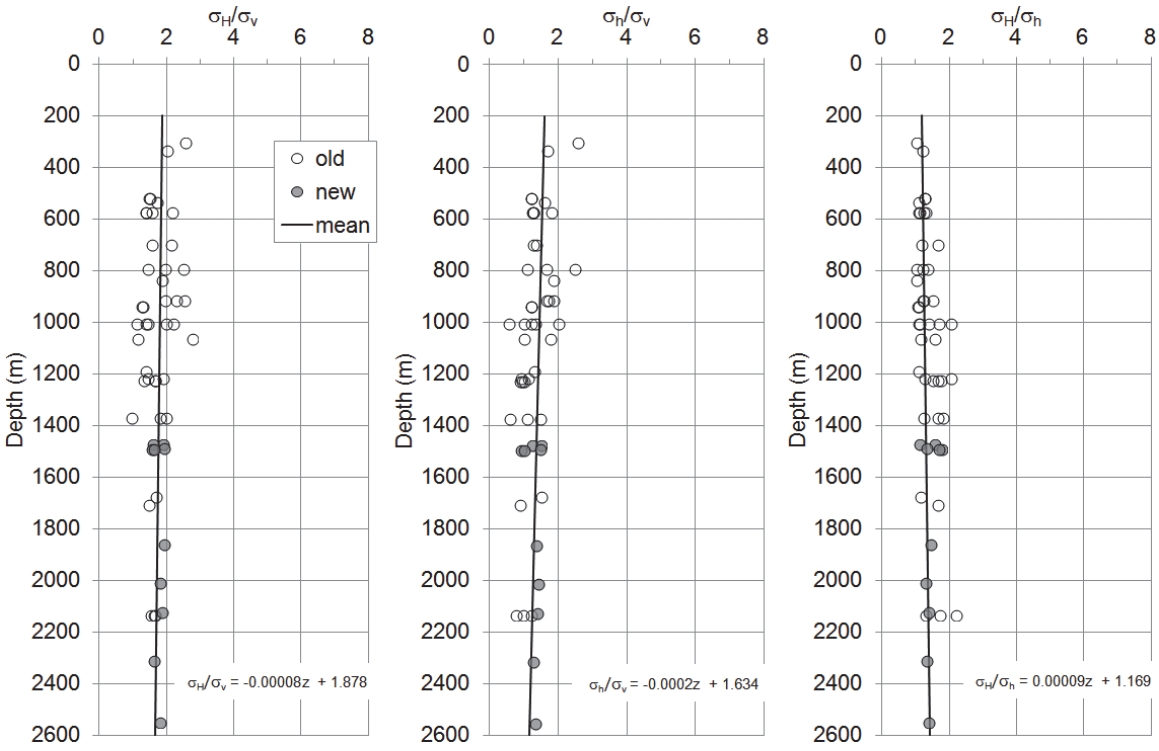

Figure 18: Horizontal and Vertical Stress Ratios for the Southern Province

4.3 DATA UNCERTAINTY

Uncertainty in constraining the in-situ stress tensor based on field measurements can be attributed to a number of sources related to experimental error (glue or instrument issues, installation or procedural errors, etc.) or analysis error (selection of final strains or displacements or material properties, assumptions associated with specific techniques, etc.). Although the data quality was assessed in this study, it is not possible to completely eliminate either source of error in the current database. The best-fit relationships were developed based on the quality assessment and the definition of uncertainty in this discussion is measured against this “best” estimate.

The distributions of the deviation of the database from the mean best-fit relationships are plotted in Figure 19, according to depth domains and geological setting. This allows for a relative assessment of the uncertainty within the database as defined by the width and symmetry of the curves, as well as the distance of the curve peaks from the mean. Relative precision is indicated by the width of the curve: tall and narrow define high precision while squat and wide indicates low precision. The symmetry of the curve provides an idea of the skewness and the tendency of results to be above or below the mean. The distance of curve peak from the mean is an indicator of either the presence of appreciable systematic errors and/or a sample population insufficient for minimising random errors.

Regressions of the best quality data for Domain 2 and depths greater than 1,500 m were completed to ascertain the mean for the purpose of assessing the uncertainty in this section. However, the results confirm that development of best-fit relationships would not be robustly constrained for these depth domains.

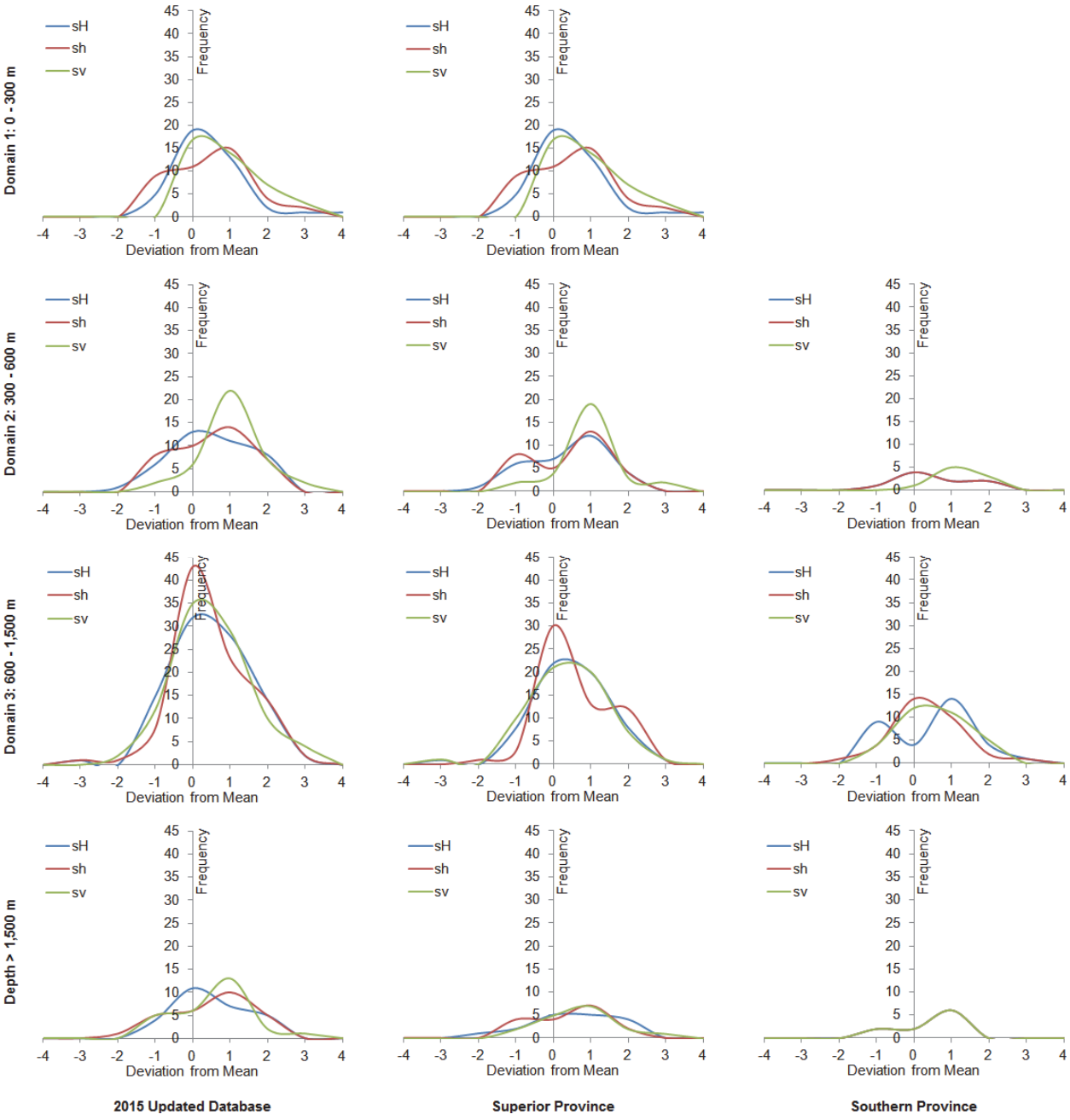

Figure 19: Distribution of Horizontal and Vertical Stress Deviation from Best-fit Relationships

Curves for the three Cartesian stress components of Domain 3 indicate that this domain, regardless of geological setting, is the best constrained. The curves are relatively narrow and the peaks are centered about the mean. The uncertainty increases when the distributions are separated into geological provinces. In both cases, σ_v remains well-constrained with a unimodal characteristic. A bimodal character takes form in σ_h of the Superior Province and σ_h of the Southern Province. There is a general positive skew to the curves and the Southern Province is

not as well constrained as the Superior Province. This is most likely due to a small number of measurements made in the Southern Province.

In Domain 1, which represent only the Superior Province, the maximum horizontal and vertical stress components are better constrained than the minimum horizontal stress. This has been evident throughout this study. There is generally more scatter in the magnitude and orientation data of σ_h.

Interestingly, the number of data in Domains 1 and 2 differ by only two points but the stress components of the stress-relaxed Domain 1 appear to be better constrained than transitional Domain 2. The peak of σ_v is consistently centered about one deviation from the mean in Domain 2. In addition, a bimodal nature appears in the Superior Province for both horizontal stress components. The uncertainty of the horizontal stress components in the Southern Province are equivalent in distribution and lie on top of one another.

Although measurement data available for depths greater than 1,500 m is half of that for Domain 2, the characteristics of the three Cartesian stress components are similar and show greater uncertainty in the mean estimate for this depth range. In the Southern Province, the distributions of all three components are equivalent and lie atop each other.

5. CONCLUSIONS

The focus of this report has been to provide a reasoned interpretation of the stress determination data compiled for this review. The 2005 database included 229 entries and 75 were added in the 2015 review for a total of 304 entries. As a result of the data quality assessment, the current 2015 database encompasses 199 entries, consisting of 173 from the 2005 review and 26 additions. The best-fit relationships (summarised below) developed in this study also focused on the depth domains Domains 1 (0 to 300 m) and 3 (600 to 1500 m) that would provide the most robust interpretation (data volume and regression characteristics). Variability and uncertainty has been shown in this study to be highest in the transitional stress Domain 2 (300 to 600 m depths).

Domain 1	Domain 3
σ_H (MPa) = (0.060±0.027)z* + (3.722±4.659)	σ_H (MPa) = (0.035±0.005)z* + (9.500±5.373)
σ_h (MPa) = (0.044±0.022)z* + (2.981±3.766)	σ_h (MPa) = (0.024±0.005)z* + (8.883±4.867)
σ_v (MPa) = (0.026±0.002)z*	

*depth in metres

While this review will provide insights for the initial phases of a siting program, direct measurements of ground stress magnitudes and orientations would be required to provide a more reliable means to constrain the stress state and to reduce uncertainty in the design and performance assessment of a DGR.

ACKNOWLEDGEMENTS

For their contributions to this review, the authors thank: John Henning of Goldcorp; Brad Simser and Dave Counter of Glencore; Bryan Wilson of North American Palladium; Mike Yao, Wei Wei, and Dave Landry of Vale; Gordon Skrecky of Aurico Gold; and Peter Kaiser of GeoK.

REFERENCES

Amadei, B. and O. Stephason. 1997. Rock Stress and Its Measurement. Chapman and Hall, London.

Kaiser, P.K. and S. Maloney. 2005. Review of ground stress database for the Canadian Shield. OPG Report No. 06819-REP-01300-10107-ROO.

Reinecker, J., B. Sperner, B. Tingay and F. Wenzel. 2004. Stress maps in a minute: The 2004 World Stress Map. Release. Eos Transactions 85(49), 521-529.

APPENDIX A: IN SITU STRESS DATABASE

Site	Depth (m)	σ_1 (MPa)			σ_2 (MPa)			σ_3 (MPa)			σ_v (MPa)	Geological Province	Rock Type	Method	E (GPa)
		Mag	Tre	Plu	Mag	Tre	Plu	Mag	Tre	Plu					
#3shaft	2001	94.7	249	54	54.4	6	18	14.4	106	30	71.2	Superior	Rhyolite	Doorstopper	85
Ansil	1220	53.2	226	10	19.4	7	77	10.8	135	8	20.3	Superior	Andesite	BH Slotter	96
Ansil	1220	40.6	232	1	25.2	141	49	15.7	324	41	21.1	Superior	Andesite	BH Slotter	96
Ansil	1340	58.9	281	4	44.2	13	29	22.9	183	61	28.1	Superior	Andesite	BH Slotter	96
Birchtree	457	42.5	17	6	23.9	108	17	16.9	267	72	17.8	Superior	Schist	Doorstopper	-
Birchtree	838	31.7	289	14	26.8	22	6	15.0	139	75	16.1	Superior	Schist	Doorstopper	-
Bousquet	190	19.1	35	0	14.4	125	11	7.2	303	79	7.4	Superior	Tuff	CSIR Triaxial	47
Bousquet	190	14.3	34	6	7.0	303	12	4.8	152	76	5.0	Superior	Tuff	CSIR Triaxial	47
Bousquet	190	16.7	45	0	10.8	135	0	6.0	135	90	6.2	Superior	unknown	unknown	-
Campbell	580	26.2	78	5	16.9	344	38	2.6	174	52	8.2	Superior	Andesite	CSIR Triaxial	74.3
Campbell	580	30.8	74	8	18.6	340	26	5.1	179	62	8.3	Superior	Andesite	CSIR Triaxial	74.3
Campbell	625	23.2	195	13	9.5	86	55	7.5	293	31	9.7	Superior	Andesite	CSIR Triaxial	91.7
Campbell	625	22.2	74	35	15.0	183	25	9.2	300	45	14.5	Superior	Andesite	CSIR Triaxial	91.7
Campbell	625	23.8	67	2	15.7	336	18	10.2	162	72	10.8	Superior	Andesite	CSIR Triaxial	91.7
Campbell	625	40.8	217	15	17.9	42	75	9.5	307	1	19.4	Superior	Andesite	CSIR Triaxial	90.5
Campbell	625	24.0	141	15	16.1	46	17	9.8	270	67	11.3	Superior	Andesite	CSIR Triaxial	90.5
Campbell	625	24.5	56	38	17.2	258	49	3.9	155	11	19.5	Superior	Andesite	CSIR Triaxial	86.5
Campbell	670	62.2	317	24	30.6	58	23	16.6	185	55	26.5	Superior	Andesite	CSIR Triaxial	83.5
Campbell	670	41.7	91	9	25.0	190	44	10.0	352	44	18.1	Superior	Andesite	CSIR Triaxial	83.5
Campbell	990	49.8	58	17	26.2	321	23	10.9	180	61	16.5	Superior	Andesite	CSIR Triaxial	85.3
Campbell	990	41.6	86	10	19.0	351	26	15.3	195	62	18.4	Superior	Andesite	CSIR Triaxial	85.3
Campbell	1220	67.4	246	27	39.3	341	11	30.1	92	61	37.9	Superior	Andesite	CSIR Triaxial	84.8
Campbell	1220	74.1	238	30	43.5	336	12	32.6	85	57	43.7	Superior	Andesite	CSIR Triaxial	85
Campbell	1220	81.6	254	1	40.7	345	31	14.1	162	59	21.2	Superior	Andesite	CSIR/CSIRO Triaxial	85
Campbell	1650	81.6	235	34	60.0	129	22	23.9	13	47	46.7	Superior	unknown	Doorstopper	-
Campbell	1785	80.5	235	11	68.6	132	47	38.4	335	41	56.2	Superior	unknown	Doorstopper	-
Casa Berardi	360	22.0	75	17	12.7	171	17	10.6	302	65	11.7	Superior	Siltstone	Doorstopper	-
Casa Berardi	430	8.6	265	37	8.2	172	5	5.8	76	52	6.8	Superior	Siltstone	Doorstopper	-
Chimo	710	51.9	7	20	31.8	100	7	16.1	206	67	21.0	Superior	Andesite	CSIR Biaxial	71.7
Chimo	780	42.3	46	22	21.3	315	5	18.9	215	67	22.1	Superior	Andesite	CSIR Triaxial	-
Chimo	780	47.0	10	3	28.6	100	6	22.6	284	84	22.8	Superior	Andesite	CSIR Triaxial	-
Cochenour	1600	46.1	181	14	36.0	44	71	22.9	274	13	36.0	Superior	Basalt	CSIRO HI	113
Cochenour	1600	64.9	111	32	40.3	214	20	24.4	330	51	37.8	Superior	Basalt & Lamprophyre Dyke	USBM	48-93
Copper Cliff N	914	43.6	246	7	23.7	155	12	14.9	5	76	15.7	Southern	unknown	CSIRO HI	-
Copper Cliff N	914	42.0	232	5	22.2	140	20	16.6	335	70	17.6	Southern	unknown	CSIRO HI	-
Copper Cliff N	914	43.1	241	3	28.9	151	13	16.5	344	77	17.2	Southern	unknown	CSIRO HI	-
Copper Rand	806	42.9	241	2	29.2	341	77	19.8	150	12	28.8	Superior	unknown	CSIRO HI	-
Copper Rand	1078	36.0	68	7	27.8	337	6	21.8	205	81	21.1	Superior	unknown	CSIRO HI	-
Copper Rand	1078	63.7	275	4	35.0	7	16	29.6	172	74	30.1	Superior	unknown	CSIRO HI	-
Corbet	665	47.4	47	0	32.9	137	0	17.8	0	90	17.9	Superior	unknown	CSIRO HI	84.8
Creighton	701	38.0	300	25	27.0	32	5	16.4	128	66	20.7	Southern	Gabbro	CSIR Triaxial	-
Creighton	1219	60.3	250	13	45.7	348	35	34.3	144	52	39.4	Southern	Gabbro	CSIR Triaxial	-
Creighton	1219	34.5	92	12	20.5	348	47	13.3	194	40	18.0	Southern	Gabbro	CSIR Triaxial	-
Creighton	1707	84.1	248	7	53.9	133	73	40.5	340	15	53.3	Southern	Gabbro	CSIR Triaxial	-
Creighton	2134	61.4	265	8	37.1	142	74	26.8	358	13	36.8	Southern	Schist	CSIR Triaxial	-
Creighton	2134	63.9	266	22	39.2	159	35	28.8	22	46	36.8	Southern	Schist	CSIR Triaxial	-
Creighton	2134	78.6	274	22	65.9	17	26	39.2	149	54	49.4	Southern	Gabbro	Doorstopper	-
David Bell	1000	44.6	4	23	25.6	100	14	23.5	218	62	26.6	Superior	unknown	CSIRO HI	-
David Bell	1000	34.7	359	10	25.5	267	9	18.5	137	76	19.1	Superior	unknown	CSIRO HI	-
Denison	305	36.5	45	0	20.0	135	0	11.0	0	90	11.0	Southern	Quartzite	Doorstopper	-
Denison	701	36.5	90	0	22.0	0	0	17.2	0	90	17.2	Southern	Quartzite	Doorstopper	-
Denison	939	30.6	318	11	21.6	206	63	16.2	53	16	19.5	Southern	Quartzite	CSIRO HI	-
Denison	939	31.5	40	25	26.0	306	6	20.0	205	65	22.3	Southern	Quartzite	CSIRO HI	-
Detour Lake	60	4.0	257	32	2.0	348	2	0.6	82	58	1.5	Superior	Basalt	CSIR Biaxial	65.7
Dome	438	18.0	215	32	15.1	113	18	9.2	358	52	12.2	Superior	Porphyry	CSIR Triaxial	59.8
Dome	438	19.5	249	32	19.1	143	28	7.0	16	48	12.4	Superior	Porphyry	CSIR Triaxial	59.8
Dome	937	42.8	63	2	28.4	157	67	20.9	332	23	27.2	Superior	Greenstone	CSIR Triaxial	63.3
Dome	937	45.5	239	26	28.5	114	49	18.2	345	28	29.5	Superior	Greenstone	CSIR Triaxial	63.3
Dome	1238	53.3	273	1	35.5	183	21	23.8	5	69	25.3	Superior	Greenstone	CSIR Triaxial	65.6
Dome	1238	52.0	249	8	42.5	158	10	27.2	17	77	28.2	Superior	Greenstone	CSIR Triaxial	65.6
Doyon	570	43.7	196	1	25.4	106	17	15.6	291	72	16.3	Superior	Andesite	CSIR Triaxial	-
Doyon	570	37.8	356	3	28.8	87	12	17.4	248	77	17.9	Superior	Andesite	CSIR Triaxial	-
Doyon	686	40.5	224	18	36.6	133	3	20.0	33	72	22.1	Superior	Andesite	Doorstopper	-
Dumagami/LaRonde	900	51.8	46	0	35.8	136	3	19.0	300	86	19.1	Superior	Tuff	CSIR Triaxial	53.1
Dumagami/LaRonde	900	57.2	44	21	36.8	138	11	10.5	256	66	17.7	Superior	Tuff	CSIR Triaxial	66.89
Dumagami/LaRonde	900	63.8	24	11	43.2	115	5	14.3	227	77	16.6	Superior	Tuff	CSIR Triaxial	66.89
Dumagami/LaRonde	1460	59.2	26	20	48.2	281	35	24.4	140	48	35.9	Superior	unknown	Doorstopper	-

Site	Depth (m)	σ_1 (MPa)			σ_2 (MPa)			σ_3 (MPa)			σ_v (MPa)	Geological Province	Rock Type	Method	E (GPa)
		Mag	Tre	Plu	Mag	Tre	Plu	Mag	Tre	Plu					
Dumagami/LaRonde	1500	70.8	150	14	62.8	52	29	49.7	262	58	54.1	Superior	unknown	Doorstopper	-
Eldrich-Flavel	115	12.3	79	18	6.3	340	26	1.2	200	58	3.1	Superior	Tonalite	CSIR Triaxial	69
Eldrich-Flavel	115	9.4	294	6	6.1	25	15	3.3	184	74	3.5	Superior	Tonalite	CSIR Triaxial	69
Eldrich-Flavel	276	22.2	275	18	9.0	9	11	5.7	129	69	7.4	Superior	Tonalite	CSIR Triaxial	69
Eldrich-Flavel	276	19.6	62	8	11.1	326	35	2.7	164	54	5.8	Superior	Tonalite	CSIR Triaxial	69
Francoeur	687	21.9	230	5	13.4	320	10	10.2	113	79	10.4	Superior	unknown	unknown	-
Fraser	1006	35.8	27	18	22.1	130	35	9.0	275	50	16.0	Southern	unknown	CSIRO HI	-
Fraser	1006	62.9	113	30	44.4	219	25	29.7	342	49	40.6	Southern	unknown	CSIRO HI	-
Fraser	1006	42.6	21	28	30.8	188	62	15.4	288	6	33.6	Southern	unknown	CSIRO HI	-
Fraser	1006	23.3	50	22	19.4	316	9	13.3	206	66	14.8	Southern	unknown	CSIRO HI	-
Fraser	1006	32.7	46	20	20.1	311	16	7.6	185	65	11.6	Southern	unknown	CSIRO HI	-
Fraser	1372	55.0	250	55	45.1	105	30	27.0	5	17	50.5	Southern	unknown	CSIRO HI	-
Fraser	1372	63.1	277	2	37.4	185	36	28.5	9	54	31.7	Southern	unknown	CSIRO HI	-
Garson	1493.5	72.8	74	9	45.4	184	66	35.0	340	22	44.5	Southern	Norite	CSIRO HI	81.4
Garson	1493.5	83.0	253	2	48.6	149	83	44.3	343	7	48.6	Southern	Norite	CSIRO HI	82.1
Golden Giant	1432	19.8	92	47	13.1	236	38	10.5	341	18	16.6	Superior	unknown	BH Slotter	-
Holt-McDermott	650	33.1	300	1	32.0	210	6	17.6	224	84	17.8	Superior	Basalt	USBM	88.05
Isle Dieu	430	32.5	202	10	13.0	306	56	9.7	106	32	12.6	Superior	Rhyolite	BH Slotter	109
Joe Mann	365	26.4	236	2	13.8	145	22	11.1	332	68	11.5	Superior	Gabbro	CSIR Triaxial	73.1
Joe Mann	365	25.0	228	3	11.3	127	73	10.2	320	15	11.3	Superior	Gabbro	CSIR Triaxial	73.1
Joe Mann	556	28.9	178	4	17.4	85	14	11.6	288	74	12.1	Superior	Gabbro	CSIR Triaxial	42.6
Joe Mann	716	51.2	330	2	44.8	61	13	20.1	230	77	21.4	Superior	Gabbro	CSIR Triaxial	102
Kidd Creek	488	33.1	94	6	26.8	186	23	10.3	350	60	13.4	Superior	Andesite	CSIR Biaxial	95.8
Kidd Creek	732	38.3	258	25	32.8	2	27	8.4	133	52	18.7	Superior	Rhyolite	CSIR Triaxial	65
Kidd Creek	732	59.5	95	18	33.0	2	8	17.9	261	70	22.2	Superior	Rhyolite	CSIR Triaxial	65
Kidd Creek	853	53.4	250	10	51.9	342	9	19.1	112	77	20.9	Superior	Diorite	CSIR Biaxial	95.8
Kidd Creek	853	53.2	77	12	39.9	170	18	16.3	318	70	23.6	Superior	Diorite	CSIR Triaxial	77.9
Kidd Creek	853	67.9	86	16	48.6	355	10	28.1	236	72	34.6	Superior	Andesite	CSIR/CSIRO Triaxial	96
Kidd Creek	1041	54.8	353	13	36.2	263	1	33.2	170	77	34.4	Superior	Andesite	CSIR Biaxial	96.5
Kidd Creek	1382	69.4	126	24	31.7	271	62	25.5	29	14	37.6	Superior	Andesite	CSIR Triaxial	87.9
Kidd Creek	1382	74.1	91	16	41.8	354	24	27.2	211	61	33.0	Superior	Andesite	CSIR Triaxial	87.9
Kidd Creek	2064	86.4	20	10	48.5	131	61	33.9	285	26	47.0	Superior	Andesite/Diorite	CSIR Triaxial	86.36
Kidd Creek	2064	78.9	38	15	59.8	129	6	54.1	237	74	55.9	Superior	Andesite/Diorite	CSIR Triaxial	86.9
Kidd Creek	2064	86.1	17	14	56.0	109	8	41.1	229	73	44.2	Superior	Andesite/Diorite	CSIR Triaxial	88
Kidd Creek	2064	97.0	66	31	56.8	167	17	38.7	282	53	56.0	Superior	Andesite/Diorite	CSIR Triaxial	86.75
Kidd Creek	2064	88.1	234	24	53.6	343	35	30.1	118	44	47.9	Superior	Andesite/Diorite	CSIR Triaxial	86.75
Kiena	170	4.7	207	10	1.4	302	24	1.3	95	64	1.3	Superior	Breccia	CSIRO HI	45.8
Kiena	170	8.1	32	1	3.5	302	11	2.7	122	79	2.7	Superior	Breccia	CSIRO HI	55.2
Kiena	170	7.9	195	3	4.4	105	3	2.6	325	85	2.6	Superior	Breccia	CSIRO HI	55.8
Kiena	170	9.9	254	13	6.2	344	4	2.2	92	77	2.4	Superior	Breccia	CSIRO HI	63.8
Kiena	273	13.1	59	5	8.0	151	20	4.9	316	69	5.3	Superior	Breccia	CSIRO HI	63.2
Kiena	810	61.2	206	2	44.9	296	2	26.0	346	87	26.0	Superior	unknown	unknown	-
Lac des Iles	645	40.3	274	9	23.7	10	34	18.1	170	55	20.4	Superior	Gabbro	CSIRO HI	96.33292
Lac Shortt	39	15.0	321	3	11.2	52	13	3.6	218	77	4.0	Superior	unknown	CSIRO HI	-
Lac Shortt	39	12.8	322	3	8.1	53	9	5.2	214	81	5.3	Superior	unknown	CSIRO HI	-
Lac Shortt	132	34.0	100	14	18.8	192	8	10.5	312	74	10.5	Superior	unknown	CSIRO HI	54.6
Lockerby	518	22.5	239	10	13.9	336	34	12.7	135	54	13.3	Southern	unknown	CSIRO HI	-
Lockerby	518	22.7	334	31	22.2	250	7	12.8	148	58	15.6	Southern	unknown	CSIRO HI	-
Lockerby	572	35.2	262	19	26.3	359	18	18.7	129	63	21.1	Southern	unknown	CSIRO HI	-
Lockerby	572	39.6	237	16	29.9	328	2	24.4	63	74	25.6	Southern	unknown	CSIRO HI	-
Lockerby	572	28.7	244	18	20.2	153	3	10.1	56	72	11.9	Southern	unknown	CSIRO HI	-
Lockerby	572	25.2	166	19	21.5	259	9	15.9	13	70	17.2	Southern	unknown	CSIRO HI	-
Lockerby	792	37.2	268	21	26.6	173	12	21.9	55	66	24.2	Southern	unknown	CSIRO HI	-
Lockerby	792	39.9	322	3	37.6	52	5	15.3	204	84	15.5	Southern	unknown	CSIRO HI	-
Lockerby	792	39.9	304	14	23.7	214	0	15.8	123	76	17.2	Southern	unknown	CSIRO HI	-
Louvicourt	855	35.3	249	27	27.6	343	9	3.3	90	61	10.7	Superior	unknown	unknown	-
Macassa	1440	55.1	325	28	34.1	228	12	29.3	116	58	35.3	Superior	Tuff	CSIR Triaxial	69
Macassa	1440	58.5	124	3	37.6	214	27	32.2	35	63	33.5	Superior	Tuff	CSIR Triaxial	69
Macassa	1440	66.9	348	8	38.5	254	25	35.8	95	63	37.0	Superior	Tuff	CSIR Triaxial	69
Macassa	1585	54.1	168	10	33.6	261	16	29.2	46	71	30.3	Superior	Syenite	CSIRO HI	64
Macassa	1890	83.2	359	16	61.8	265	13	47.5	138	70	50.8	Superior	Syenite	CSIRO HI	68.6
Macassa	1890	76.0	21	18	36.1	280	30	28.5	137	54	35.2	Superior	Syenite	CSIRO HI	69
Macassa	1890	88.6	12	24	67.1	280	5	40.2	178	66	48.4	Superior	Syenite	CSIRO HI	68.6
Macassa	2005	75.0	357	17	57.6	198	68	32.6	90	7	59.2	Superior	Syenite	CSIR Triaxial	66.6
Macassa	2005	84.2	8	32	61.3	123	33	44.0	246	40	60.7	Superior	Syenite	CSIR Triaxial	66.6
MacLeod	366	42.5	133	33	34.3	229	9	15.1	332	56	23.8	Superior	Tuff	CSIR Triaxial	-
MacLeod	479	30.0	251	11	27.7	343	8	18.7	110	76	19.2	Superior	Diorite	Doorstopper	-
MacLeod	545	17.4	355	63	13.4	233	15	8.8	136	22	15.9	Superior	unknown	CSIR Triaxial	-
MacLeod	545	20.9	343	63	16.2	249	2	5.5	158	27	17.7	Superior	unknown	CSIR Triaxial	-
MacLeod	570	47.2	222	17	34.1	315	9	26.7	70	70	28.4	Superior	Tuff	Doorstopper	-
MacLeod	570	31.6	162	11	27.9	70	12	21.5	295	74	22.2	Superior	Tuff	Doorstopper	-

Site	Depth (m)	σ_1 (MPa)			σ_2 (MPa)			σ_3 (MPa)			σ_v (MPa)	Geological Province	Rock Type	Method	E (GPa)
		Mag	Tre	Plu	Mag	Tre	Plu	Mag	Tre	Plu					
MacLeod	570	38.3	356	22	29.5	90	11	21.4	206	66	24.3	Superior	Tuff	Doorstopper	-
MacLeod	570	19.9	224	4	16.6	315	6	14.6	100	83	14.7	Superior	Tuff	Doorstopper	-
MacLeod	788	24.4	148	17	21.1	45	35	13.9	260	50	17.2	Superior	unknown	CSIR Triaxial	-
Musselwhite	740	35.5	280	8	21.5	12	16	18.2	162	72	18.8	Superior	Schist	CSIRO HI	97.6
Musselwhite	740	45.2	270	4	18.6	0	8	18.1	153	81	18.2	Superior	Schist	CSIRO HI	96.2
Musselwhite	740	39.6	274	2	28.4	183	12	13.2	15	78	13.9	Superior	Schist	CSIRO HI	91.7
Nickel Rim South	1475	60.6	103	5	38.4	11	25	29.4	203	64	31.2	Southern	Norite	CSIRO HI	-
Nickel Rim South	1475	57.4	124	3	50.3	35	26	30.1	209	63	34.2	Southern	Norite	CSIRO HI	52.46
Nordic	335	20.7	90	0	17.2	0	0	10.3	0	90	10.3	Southern	Quartzite	Doorstopper/CSIR Triaxial	-
Onaping	1227	67.0	267	20	39.8	15	32	32.8	151	51	38.8	Southern	Norite	CSIR Triaxial	-
Onaping	1227	59.0	264	22	33.4	2	18	28.2	127	61	33.0	Southern	Norite	CSIR Triaxial	-
Onaping	1227	67.5	260	26	44.6	23	48	37.1	154	30	46.9	Southern	Norite	CSIR Triaxial	-
Onaping	1372	84.5	240	9	50.3	334	12	40.7	122	72	41.1	Southern	Norite	CSIRO HI	-
Onaping	1488	77.0	163	4	56.0	254	18	37.0	61	71	39.3	Southern	Felsic Norite	AE	-
Onaping	1676	81.4	223	9	48.3	320	27	35.5	115	62	39.6	Southern	Norite	CSIRO HI	-
Onaping	1861	96.0	174	4	67.0	265	13	48.0	65	77	49.3	Southern	Felsic Norite	AE	-
Onaping	2012	100.0	169	3	76.0	260	8	54.0	57	81	55.3	Southern	Felsic Norite	AE	-
Onaping	2123	109.0	184	1	80.0	94	5	58.0	286	85	57.7	Southern	Felsic Norite	AE	-
Onaping	2311	111.0	178	18	83.0	273	17	57.0	44	65	64.0	Southern	Felsic Norite	AE	-
Onaping	2552	129.0	190	8	92.0	100	1	69.0	1	82	69.6	Southern	Felsic Gneiss	AE	-
Red Lake HGZ	1807	74.3	314	33	55.7	204	28	28.6	82	44	48.0	Superior	Rhyolite	Doorstopper	88.333
Selbaie	70	3.4	165	19	1.4	15	68	-0.5	258	10	1.6	Superior	Dacite	CSIRO HI	62.8
Selbaie	180	6.9	312	10	3.3	34	1	1.8	128	80	2.0	Superior	Dacite	CSIRO HI	69.7
Selbaie	180	11.7	304	4	4.3	214	3	2.0	90	85	2.1	Superior	Dacite	CSIRO HI	69.7
Selbaie	180	11.7	132	3	6.8	227	57	6.6	40	34	6.6	Superior	Dacite	CSIRO HI	69.7
Sigma	1142	47.1	9	11	35.3	268	41	24.7	112	46	30.3	Superior	Porphyry	CSIR Triaxial	74.5
Stanleigh	1066	34.2	196	33	29.6	300	20	25.0	56	50	28.2	Southern	Quartzite	CSIRO HI	75.5
Stanleigh	1066	62.9	253	11	35.9	162	5	19.8	48	78	21.5	Southern	Quartzite	CSIRO HI	75.5
Strathcona	533	38.6	128	21	34.5	31	18	16.6	264	61	21.0	Southern	Norite	CSIRO HI	-
Strathcona	838	60.0	314	1	55.8	44	4	31.0	206	86	31.1	Southern	Granite	CSIRO HI	-
Strathcona	1190	50.6	295	16	44.0	203	8	33.0	87	72	34.5	Southern	unknown	CSIRO HI	-
Thompson	610	58.5	323	11	40.5	61	32	18.3	214	54	25.5	Superior	Gneiss	Doorstopper	-
URL	12	8.6	207	2	5.1	117	0	1.1	27	88	1.1	Superior	Granite	CSIR Triaxial	-
URL	61	7.4	43	25	4.5	306	14	1.6	189	60	2.8	Superior	Granite	CSIR Triaxial	-
URL	61	7.4	40	31	3.4	304	9	1.1	199	58	2.8	Superior	Granite	CSIR Triaxial	-
URL	61	7.3	57	32	5.0	316	18	1.1	201	53	3.2	Superior	Granite	CSIR Triaxial	-
URL	61	6.5	44	24	3.7	309	11	1.0	195	64	2.0	Superior	Granite	CSIR Triaxial	-
URL	128	13.8	206	8	8.3	116	1	3.5	20	82	3.7	Superior	Granite	CSIR Triaxial	-
URL	129	12.8	194	8	9.1	103	11	6.1	317	77	6.4	Superior	Granite	CSIR Triaxial	-
URL	129	16.7	181	10	9.6	88	18	6.4	298	70	7.1	Superior	Granite	CSIR Triaxial	-
URL	129	13.0	50	12	8.3	303	52	5.5	149	35	7.5	Superior	Granite	CSIR Triaxial	-
URL	183	16.2	165	44	12.1	330	45	4.9	67	7	13.9	Superior	Granite	CSIR Triaxial	-
URL	183	14.8	219	3	12.9	309	12	6.6	115	78	6.9	Superior	Granite	CSIR Triaxial	-
URL	183	13.1	213	5	11.1	304	9	6.1	95	80	6.3	Superior	Granite	CSIR Triaxial	-
URL	183	16.8	233	23	11.3	325	5	9.0	67	66	10.2	Superior	Granite	CSIR Triaxial	-
URL	235	29.2	214	23	11.9	115	22	10.1	346	58	13.4	Superior	Granite	CSIR Triaxial	-
URL	235	31.5	219	20	12.2	70	67	10.4	313	11	14.4	Superior	Granite	CSIR Triaxial	-
URL	235	25.5	228	41	13.3	104	32	12.3	351	32	18.2	Superior	Granite	CSIR Triaxial	-
URL	235	26.8	233	29	17.4	124	30	14.0	357	46	17.9	Superior	Granite	CSIR Triaxial	-
URL	235	26.6	218	63	21.6	119	4	14.6	27	27	24.2	Superior	Granite	CSIR Triaxial	-
URL	235	36.0	230	31	25.1	118	32	16.8	354	42	24.1	Superior	Granite	CSIR Triaxial	-
URL	235	28.0	240	53	18.7	118	21	14.6	16	28	23.5	Superior	Granite	CSIR Triaxial	-
URL	235	31.1	65	16	18.4	161	21	15.4	300	64	17.2	Superior	Granite	CSIR Triaxial	-
URL	416	45.4	69	6	31.0	159	3	14.9	276	84	15.3	Superior	Granite	CSIR Triaxial	-
URL	417	43.9	74	3	27.2	164	7	14.9	325	82	15.1	Superior	Granite	CSIR Triaxial	-
URL	417	49.0	57	3	31.1	148	15	13.2	316	75	14.5	Superior	Granite	CSIR Triaxial	-
URL	417	48.7	22	1	31.6	112	7	14.3	285	83	14.6	Superior	Granite	CSIR Triaxial	-
URL	417	54.7	162	3	22.2	70	24	13.6	258	66	15.2	Superior	Granite	CSIR Triaxial	-
URL	417	48.3	150	4	26.3	59	14	13.6	257	76	14.6	Superior	Granite	CSIR Triaxial	-
URL	417	53.7	151	13	22.9	58	10	13.9	294	74	16.3	Superior	Granite	CSIR Triaxial	-
URL	417	41.4	16	3	30.3	107	16	12.8	276	74	14.2	Superior	Granite	CSIR Triaxial	-